CONF-8[illegible]--1

SAND 80-0857C

DYNAMIC ROCK FRAGMENTATION: OIL SHALE APPLICATIONS

R. R. Boade, D. E. Grady, and M. E. Kipp
Sandia National Laboratories
Albuquerque, New Mexico 87185

MASTER

REA

DISCLAIMER

DYNAMIC ROCK FRAGMENTATION: OIL SHALE APPLICATIONS*

R. R. Boade, D. E. Grady, and M. E. Kipp
Sandia National Laboratories
Albuquerque, New Mexico 87185

INTRODUCTION

Explosive rock fragmentation techniques used in many resource recovery operations have in the past relied heavily upon traditions of field experience for their design. As these resources, notably energy resources, become less accessible, it becomes increasingly important that fragmentation techniques be optimized and that methods be developed to effectively evaluate new or modified explosive deployment schemes. Computational procedures have significant potential in these areas, but practical applications must be preceded by a thorough understanding of the rock fracture phenomenon and the development of physically sound computational models.

This paper presents some of the important features of a rock fragmentation model that was developed as part of a program directed at the preparation of subterranean beds for in situ processing of oil shale. The model, which has been implemented in a two-dimensional Lagrangian wavecode, employs a continuum damage concept to quantify the degree of fracturing and takes into account experimental observations that fracture strength and fragment dimensions depend on tensile strain rates. The basic premises of the model are considered in the paper as well as some comparisons between calculated results and observations from blasting experiments. More detailed descriptions of the model are given in Refs. 1-3.

FRACTURE AND FRAGMENTATION MODEL

The nature of the fragmentation phenomenon in rocks, and in other materials as well, is closely linked to the loading conditions. In oil shale, for example, fracture strength and fragment dimensions depend on strain rate (see Figure 1). This dependence is due to the existence of a distribution of flaws within the material which have different characteristic dimensions and hence also are activated at various applied tensile stress levels. At low strain rates only a few of the larger flaws are activated during the early portion of load application; these grow as the load is continued and eventually coalesce, causing material failure and the termination of the flaw activation process. Because only a few flaws have been activated, the fragments are comparatively large. At higher strain rates, flaw or crack coalescence may not occur during the period of load application unless a greater number of flaws are activated; for this to be realized, the applied tensile stress level must be greater. The fracture stress at high strain rates thus is greater than at low strain rates. Fragments also are smaller at high strain rates because a greater number of flaws are activated.

The strain-rate dependence of the fragmentation phenomenon is important in explosive applications because strain rates over the entire range depicted in Figure 1 are possible. Near a typical cylindrical borehole

*This work supported by the U. S. Department of Energy

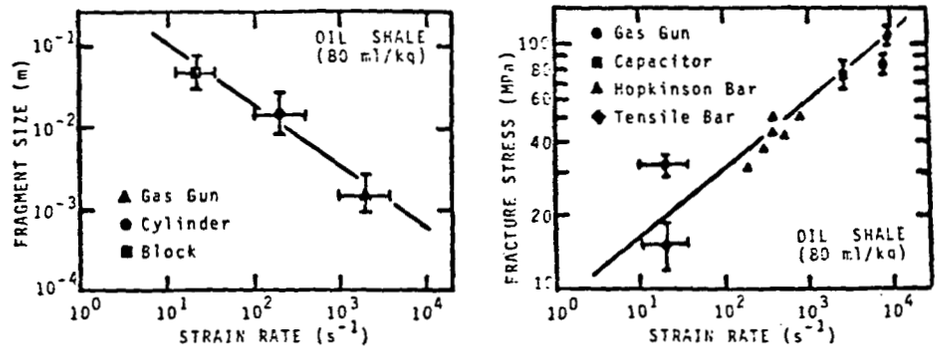

FIGURE 1. ILLUSTRATIONS OF DEPENDENCE OF FRAGMENTATION PROCESS IN OIL SHALE ON STRAIN RATE.

charge, strain rates are in the 100 - 1000 s^{-1} range; at larger radii, however, they may drop to the 1 - 10 s^{-1} range. If free faces are present, strain rates in the 1000 - 10,000 s^{-1} range may occur when tensions develop after the reflection of a compressive stress wave.

In developing the fragmentation model discussed here, the above description of the material failure process was assumed. The current state of fracture in the model is represented by a damage parameter, D, which is defined as the volume fraction of material that has lost its load carrying ability. Material strength is degraded isotropically by decreasing the bulk (K) and shear (G) moduli by a factor 1-D. In the linear elastic relations, tensile stress, σ_{ij}, is related to strain, ϵ_{ij}, by

$$\sigma_{ij} = K(1 - D)\epsilon\,\delta_{ij} + 2G(1 - D)(\epsilon_{ij} - \epsilon\,\delta_{ij}/3) , \qquad (1)$$

where $\epsilon = \epsilon_{11} + \epsilon_{22} + \epsilon_{33}$. The value of the parameter D at time t is given by

$$D(t) = \int_0^t \dot{N}(\tau)v(t - \tau)d\tau , \qquad (2)$$

where $\dot{N}$ is the rate at which flaws are activated and v is the volume of material influenced by a flaw, or crack. The number of flaws active at a given strain is described by a Wiebull distribution, $n(\epsilon) = k\epsilon^m$, where k and m are constants; $\dot{N}$ is determined from $\dot{n}$ by $\dot{N} = \dot{n}(1 - D) = km(1 - D)\epsilon^{m-1}\dot{\epsilon}$, where the 1 - D factor is included to account for flaws that are shadowed by other flaws. Assuming that a crack grows at a constant rate, C_g, and that the volume influenced by a crack is a sphere of radius $C_g t$, v is given by $4\pi(C_g t)^3/3$. Substitution into Eq. 2 for N and v yields

$$D(t) = \frac{4}{3}\pi km C_g^3 \int_0^t \epsilon^{m-1}\,\dot{\epsilon}(1 - D)(t - \tau)^3\,d\tau . \qquad (3)$$

The question of fragmentation is addressed by first assuming that the surface area of a crack at time t is $2\pi(C_g t)^2$ and that the total surface area is

$$A(t) = \int_0^t \dot{N}(\tau)a(t - \tau)d\tau = 2\pi km C_g^2 \int_0^t \epsilon^{m-1}\,\dot{\epsilon}(1 - D)(t - \tau)^2\,d\tau . \quad (4)$$

Defining an average volume at time t, $\bar{v}(t)$, and an average area, $\bar{a}(t)$, along with an average radius $\bar{r}(t)$, Eqs. 2 and 4 can be rewritten as

$$D(t) = \int_0^t \dot{N}(\tau)\bar{v}(t)d\tau = N(t)\bar{v}(t) = \frac{4}{3}\pi\bar{r}^3 N(t) \quad (5)$$

and

$$A(t) = \int_0^t \dot{N}(\tau)\bar{a}(t)d\tau = N(t)\bar{a}(t) = 2\pi\bar{r}^2 N(t) . \quad (6)$$

Eliminating $\bar{r}$ from Eqs. 5 and 6 yields

$$L(t) = [1/N(t)]^{1/3} = (9\pi/2)^{1/3} D(t)^{2/3}/A(t). \quad (7)$$

N(t) is the density of activated cracks so its reciprocal is the average volume per crack and L(t) can be considered to be the average distance between cracks, or the approximate fragment dimension.

The constants in the model were evaluated using data in Figure 1 and Eqs. 1, 3, and 4 for the special case of constant strain rate. The results are $k = 1.7(10^{27})$ m^{-3}, $m = 8$, and $C_g = 1300$ m/s. It is significant to note here that constants in the model have been based on laboratory data, not field data.

The tensile fracture and fragmentation model described in the foregoing has been incorporated into a two-dimensional Lagrangian wave propagation code called TOODY. For numerically simulating the experiments that will be discussed in the next section, the oil shale was treated as an isotropic elastic-perfectly plastic material with an initial density of 2.27 Mg/m^3, a bulk sound speed of 3000 m/s, a Poisson ratio of 0.4, and a yield strength of 200 MPa. The damage and fracture surface equations were reduced to approximate ordinary differential rate equations for integration in the wavecode. The explosive energy source was treated as an isentropic release of energy in a gas from the Chapman-Jouguet point of the explosive.

NUMERICAL SIMULATIONS

The use of wavecodes to simulate explosive blasts in rock media provides insight into the nature of the early-time stress wave propagation and the attendant fragmentation; subsequent motion of the fragments is not simulated. Several studies employing the model discussed in the previous section have been performed,[1-3] some to evaluate the model and some to obtain information about the effects of varying charge shape, charge burial depth, and detonation initiation scheme. Two representative examples are considered here; both are simulations of experimental explosive blasts in oil shale, one involving a small charge in a meter-sized block and the other a cylindrical charge in a borehole drilled into the floor of a mine.

Block Experiment - The block experiment, which is illustrated on the left side of Figure 2, involved an 80 g charge of C-4 explosive in an instrumented block of oil shale. The charge was about 0.4 m from the nearest surface which was supported on a slab of low-density foam. The foam served to contain fragments that may have been ejected but had an impedance that was negligible compared to that of the rock so that for stress wave interactions this rock surface was free. As is shown in Figure 2, the block was surrounded at all other surfaces by an impedance-matching grout to minimize effects caused by internal wave reflections.

After the shot the block was slabbed for direct examination. Fragment dimensions (shown on the right of Figure 2) were determined as a function of distance from the charge, both in the direction toward the free face (solid data bars) and in an orthogonal direction (dashed data bars). As is evident, the fragments tend to be small near the charge and to become larger at greater distances, which would be

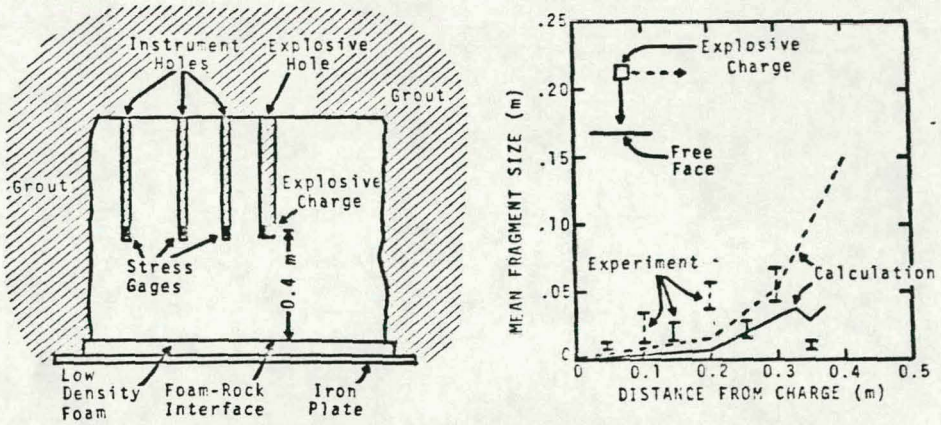

FIGURE 2. ILLUSTRATIONS OF EXPLOSIVE EXPERIMENT IN OIL SHALE BLOCK (LEFT) AND SOME OF THE FRAGMENTATION RESULTS (RIGHT).

expected since the strain rate decreases. An exception to this is the solid data bar representing fragment dimensions near the free face; fragments are small here because strain rates are high for tensile waves produced by reflection of compressive waves.

Results of the numerical simulation are also shown in Figure 2. Trends evident in the measurements are also evident in the computations. The agreement between the measurements and calculations is in general within a factor of two, which is considered reasonable in view of the relatively large spread inherent to the measured dimensions.

Mine Experiment - The mine experiment was performed in the floor of the Colony Oil Shale Mine in western Colorado by personnel from the Los Alamos National Scientific Laboratories.[4] It consisted of a 5.2 kg charge of ANFO, 0.75 m high, at the bottom of a 0.1 m diameter, 2.0 m deep borehole drilled into the floor of the mine. The charge was bottom detonated.

The blast did not result in significant ejection of fragmented material above the charge. Fragments were formed, however, but were not displaced significantly from their original locations. After the shot the loose fragments were excavated from the rock mass and profiles of the resulting crater were measured at ninety-degree intervals around the axis of the borehole. The four profiles are shown in Figure 3. There is some variation between these profiles as would be expected

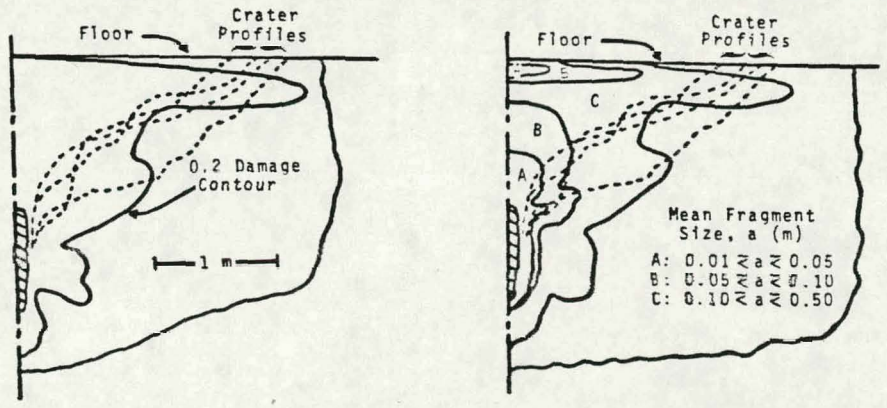

FIGURE 3. MEASURED CRATER PROFILES (DASHED) AND CALCULATED DAMAGE (LEFT) AND FRAGMENT SIZE CONTOURS (RIGHT) FOR EXPERIMENT IN MINE.

because the fragmentation process must be controlled to some extent by the joint structure of the rock medium.

One calculated damage contour is also shown in Figure 3, for D = 0.2. This contour has essentially two parts. The lower portion is due largely to the development of a tensile stress wave which trails the compressive wave induced in the rock by the detonation. The upper portion, which includes the lobe extending to the right near the floor, is due to the development of tension as the compressive wave reflects from the free face. The calculated curve is considered to be a good representation of the measured crater profiles. There are discrepancies, however, some of which can be understood by considering fragment dimensions.

The average fragment dimensions calculated for this explosive geometry are shown on the right side of Figure 3, along with the four crater profiles. The smallest fragments again appear near the charge and near the free face because of the high strains rates realized in these regions. Fragment dimensions again increase at the larger ranges. In the radial direction from the charge, the rate of increase of fragment dimensions is rather large, which would tend to make excavation from such tight quarters somewhat difficult. In addition, fragments in this region may be lodged rather firmly by residual stress fields induced by the detonation.[5] In regions above the charge and near the crater profiles, calculated fragment dimensions are comparable to spatial variations between the profiles. It is easy to hypothesize that in regions where fragments are calculated to be large, cracks may indeed form and may even surround a fragment, but may not be detected because of small displacements. It is reasonable to expect the uncertainty in a calculated, or measured, crater profile to be at least as large as the local fragment dimension.

CONCLUSIONS

Essential physical processes which affect dynamic fracture and fragmentation of rock have been incorporated into the model described in this paper. The overall agreement between calculated and experimental results is encouraging, particularly in view of the fact the the model constants were deduced from small-scale laboratory experiments and yet appear to be appropriate for larger scale field applications.

REFERENCES

1. Grady, D. E. and Kipp, M. E., "Continuum Modelling of Explosive Fracture in Oil Shale", Int. J. Rock Mech. Min. Sci. and Geomech. Abstr. Vol. 17, pp. 147-157 (1980).

2. Grady, D. E. and Kipp, M. E., "Explosive Fracture Studies in Oil Shale", to be published in Soc. Pet. Eng. J. (Oct. 1980).

3. Kipp, M. E. and Grady, D. E., Numerical Studies of Rock Fragmentation, SAND 79-1582, Sandia National Laboratories, Albuquerque, NM (1980).

4. Schmidt, S., Ed., Explosively Produced Fracture in Oil Shale, LA-8104-PR, Los Alamos National Scientific Laboratory, Los Alamos, NM (1980).

5. Schmidt, R. A., Boade, R. R., and Bass, R. R., "A New Perspective on Well Shooting - the Behavior of Contained Explosions and Deflagration", Proc. 54th Soc. Pet. Eng. Fall Tech. Conf., Las Vegas, NV (1979).